EC14026 STARS: THEORETICAL CONSIDERATIONS

G. FONTAINE, S. CHARPINET, P. BRASSARD
Département de Physique, Université de Montréal
Montréal, Québec, Canada H3C 3J7

P. CHAYER
Center for EUV Astrophysics, University of California
Berkeley, California 94720, U.S.A.

F.J. ROGERS, C.A. IGLESIAS
Lawrence Livermore National Laboratory
Livermore, California 94550, U.S.A.

AND

B. DORMAN
Laboratory for Astronomy and Solar Physics, NASA/GSFC
Greenbelt, Maryland 20771, U.S.A.

1. Introduction

The recent discovery of pulsating subdwarf B (sdB) stars at the South African Astronomical Observatory (Kilkenny et al. 1997; Koen et al. 1997; Stobie et al. 1997; O'Donoghue et al. 1997) has opened a brand new avenue in the field of asteroseismology. The study of these pulsators (dubbed EC14026 stars, after the prototype) offers the exciting possibility of exploiting the full power of asteroseismology to investigate the sdB phase of stellar evolution, one of the last frontiers in our general understanding of the history of stars.

The existence of pulsating sdB stars was predicted theoretically by Charpinet et al. (1996) as part of the first systematic investigation of the asteroseismological potential of stellar models on the extreme horizontal branch (EHB) and beyond. This was made possible thanks to significant progress in our ability to compute increasingly sophisticated and realistic models for this relatively neglected phase of stellar evolution (see Dorman 1995 for a review). Charpinet et al. (1996) uncovered an efficient driving mechanism due to an opacity bump associated with iron ionization in such models.

F.-L. Deubner et al. (eds.), New Eyes to See Inside the Sun and Stars, 367–374.

Oddly enough, both observational and theoretical efforts were carried out totally independently of each other at about the same time. The discovery of the first EC14026 stars in South Africa, however, gave our group added confidence in the basic validity of the approach of Charpinet et al. (1996). This also led us to further refinements of the physical description of the iron bump mechanism responsible for driving pulsation modes in models of sdB stars. Thus, in Charpinet et al. (1997), we demonstrated the existence of a theoretical instability strip in which all the currently known EC14026 stars fall, and obtained an excellent qualitative agreement between the periods of the expected driven modes and the observed periods. Low order radial, and low order and low degree nonradial (p and f) modes are involved. In the following, we summarize these and still more recent theoretical developments.

2. The nature of the sdB stars

It is now well established that sdB stars are evolved, compact, EHB and post–EHB objects. They are certainly evolved from the RGB, but we still do not know exactly how they are formed. The sdB stars are quite abundant in terms of surface density in shallow photographic surveys such as the Palomar–Green, Montréal–Cambridge–Tololo, and Edinburgh–Cape surveys. For instance, they dominate the population of blue objects for $V \lesssim 16$. About 300 sdB stars are brighter than $V \sim 14.3$ in the complete Palomar–Green survey.

Quantitative studies of the spectra of sdB stars (see Saffer et al. 1994 and references therein) have revealed that their atmospheric parameters are found in the ranges 40,000 K $\gtrsim T_{\rm eff} \gtrsim$ 24,000 K and $6.2 \gtrsim \log g \gtrsim 5.1$. The average values in the Saffer sample of 213 stars are $< T_{\rm eff} > \simeq 30{,}740$ K and $< \log g > \simeq 5.68$. In addition, they are all chemically peculiar. Their atmospheres are dominated by hydrogen, with helium typically underabundant by more than one order of magnitude (in number). Heavier elements (particularly C, N, and Si which have been well studied) show abundance anomalies that can be quite large (see, e.g., Heber 1991). It is believed that diffusion processes (mostly gravitational settling and radiative levitation) are at work in these stars, possibly in competition with weak stellar winds (Michaud et al. 1985).

The positions of the real sdB stars in the $T_{\rm eff}$–log g plane (or, equivalently, in the HR diagram) force their identification with low–mass ($M \lesssim 0.5\ M_{\odot}$), helium core–burning models with outer H–rich envelopes that are too thin to sustain appreciable hydrogen shell–burning on the ZAEHB. Consequently, after core helium exhaustion, these objects do not ascend the AGB; they instead turn left during their evolution in the HR diagram and, ultimately, collapse as low–mass white dwarfs. A typical evolutionary timescale for a star in the sdB phase is of order $\sim 10^8$ yr.

https://doi.org/10.1017/S0074180900238953 Published online by Cambridge University Press

3. The driving mechanism in EC14026 star models

In a first effort, Charpinet et al. (1996) investigated the pulsation properties of detailed, full evolutionary models of sdB stars with uniform solar composition in the outer H–rich envelope. Although all the modes investigated turned out to be globally stable, this led to the discovery of a region of strong local driving associated with a maximum in the Rosseland opacity in several of these models. This bump in opacity, sometimes referred to as the "Z–bump", is essentially due to the ionization of an electronic shell of iron contained in the solar mixture assumed in the stellar models. This opacity feature is sufficiently important and well located in sdB star models to produce significant local driving through the κ–effect.

Because diffusion processes are known to be at work in sdB stars (causing local overabundances –and underabundances– of a given element, depending on the location in the star), Charpinet et al. (1996) reasoned that iron could plausibly be overabundant in the driving region, thus further boosting the local opacity there. This was justified by rough radiative levitation calculations indicating that iron should indeed be overabundant in the critical region. They investigated the question with relatively crude envelope models in which the (uniform) metallicity was artificially increased beyond the solar value. Models with $Z \geq 0.04$ were found to be unstable and, on this basis, Charpinet et al. (1996) made the prediction that a subclass of sdB stars should show luminosity variations resulting from pulsational instabilities.

In a second effort, we reinvestigated the stability problem by constructing more sophisticated models in which the crude assumption of uniform metallicity has been replaced by the more realistic condition of diffusive equilibrium between gravitational settling and radiative levitation on the metal –iron– responsible for the driving process (see Charpinet et al. 1997). This necessitated detailed calculations of radiative forces on iron in the models (see, e.g., Chayer, Fontaine, & Wesemael 1995) and the computations of special OPAL opacity tables taking into account the large variations of the iron abundance about the cosmic value predicted by equilibrium radiative levitation theory.

Figure 1 illustrates some properties of these more sophisticated stratified envelope models. The solid curve in each panel gives the iron abundance as a function of fractional mass depth log q. The panels correspond to a series of representative sdB models with log $g = 5.8$ and with effective temperatures ranging from $\sim$ 22,000 K to about $\sim$ 42,000 K. Note that large overabundances of iron can be supported by radiative levitation in certain regions of the envelope of the stars, especially for the hotter models.

Associated with the nonuniform profile of iron is the run of the Rosseland opacity (dotted curve in each panel). The location and shape of the iron opacity peak are the critical factors in the efficiency of the driving process. It turns

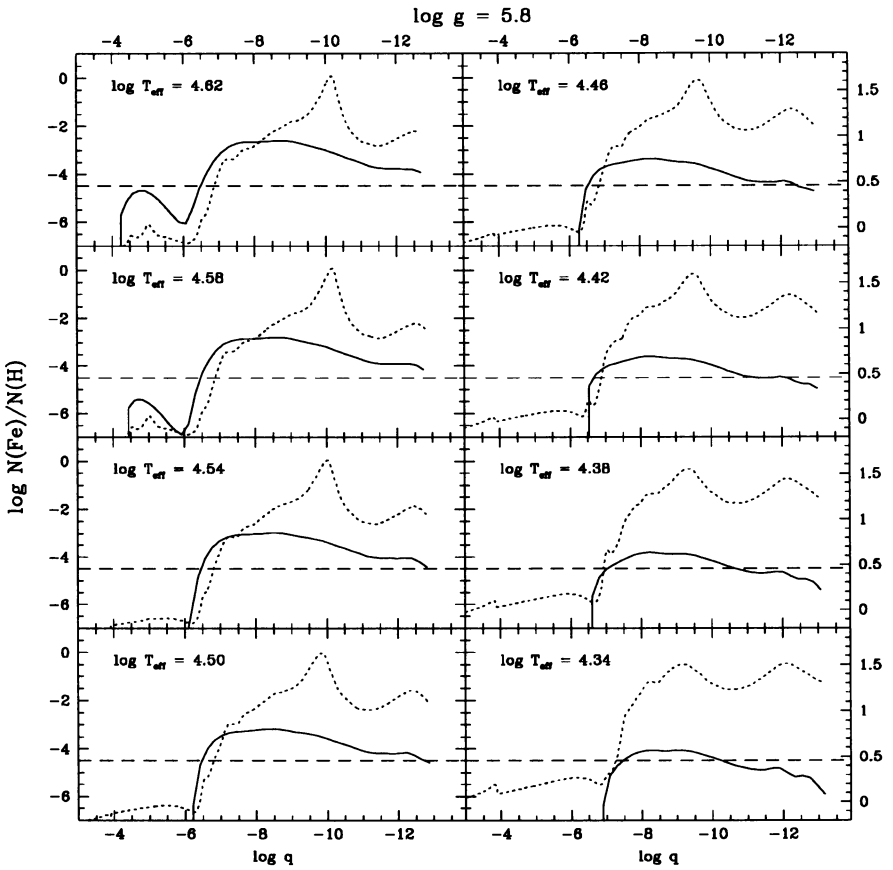

Figure 1. Equilibrium abundance of iron (solid curve) as a function of the fractional mass depth log q (= log $(1 - M(r)/M_*)$) for a series of representative models of sdB stars with $M = 0.48\ M_\odot$, log $g = 5.8$, log $q(H) = -3.70$, and log $T_{\rm eff}$ from 4.34 to 4.62 in steps of 0.04. In each panel the tip of the solid curve on the right hand side corresponds to the location of the Rosseland photosphere. The dashed horizontal line gives the normal value of the Fe/H number ratio. Also shown is the profile of the Rosseland opacity (dotted curve) whose logarithmic value can be read on the right axis.

out that, at low effective temperatures, there is not enough iron supported by radiative levitation, the iron opacity peak is rather broad and located relatively deep, and no overall driving is possible. By increasing the effective temperature, the iron opacity peak gets narrower, stronger, and moves toward the surface (the latter effect being caused by increasing overall ionization). In effect, the peak ultimately moves through the critical region for efficient driving. At too high effective temperatures, the peak has moved too far up in the envelope, past the region of efficient driving. This leads naturally to the formation of a broad instability strip.

https://doi.org/10.1017/S0074180900238953 Published online by Cambridge University Press

4. Some sample results

Figure 2 shows how the theoretical period spectrum is affected when changing the effective temperature, the 3 other free parameters of the models being kept fixed at typical values. Here, all modes with $l = 0$, 1, 2, and 3 are considered, and the period window illustrated covers the range from 80 to 280 s. The various curves refer to the fundamental modes (except for the case $l = 1$ and $k = 1$), and divide the diagram between the domain of the p–modes (below the curves) and that of the g–modes (above the curves). The excited modes define a broad instability strip in the range 39,000 K $\gtrsim$ $T_{\rm eff}$ $\gtrsim$ 27,000 K (for these log $g = 5.8$ models). Only some of the fundamental and some of the p–modes are excited; the g–modes are not driven in the present models.

Except for the f–modes and g–modes, the period of a given (p) mode is not very sensitive to $T_{\rm eff}$. However, if we focus only on the *excited* modes, the figure reveals that the iron–bump mechanism can only drive high order modes near the blue edge of the instability strip, and the lowest order modes near the red edge. Hence, we find a correlation between $T_{\rm eff}$ and excited periods such that the higher the effective temperature, the shorter the periods of the excited modes (prediction #1). In addition, the figure reveals that the largest growth rates are found for models with $T_{\rm eff} \sim$ 33,000–36,000 K. Hence, we would expect the pulsators with representative surface gravities near log $g \sim$ 5.8 to be clustered primarily around these effective temperatures (prediction #2).

Figure 3 is similar, except that, this time, the effects of varying the surface gravity are illustrated. The effective temperature, total mass, and H–rich envelope mass are now kept fixed at typical values in this second batch of models. As before, the curves divide the diagram into the domain of g–modes and that of the p–modes. Except for the odd g–mode in the lowest gravity models, the iron bump mechanism is seen to be able to excite only low order p–(and f–)modes. Physically, this is due to the fact that the p–modes are primarily envelope modes in sdB star models, while g–modes are primarily core modes with important amplitudes only in regions located much deeper than the driving region. (This distinction becomes more fuzzy in the lowest gravity models.) On the basis of our calculations, we do not expect to observe g–modes in pulsating sdB stars (prediction #3).

The figure also illustrates the large effects on the period spectrum produced by changing the surface gravity while keeping the effective temperature constant. Of course, this is no surprise here as the mechanical structure is strongly affected. The period of a given mode (i.e., for fixed values of l and k) increases substantially with decreasing surface gravity, and this is why we were forced to consider the wider range of periods, 80–800 s, in Fig. 3. The periods of the *excited* modes follow the same trend, so we expect that the lower

https://doi.org/10.1017/S0074180900238953 Published online by Cambridge University Press

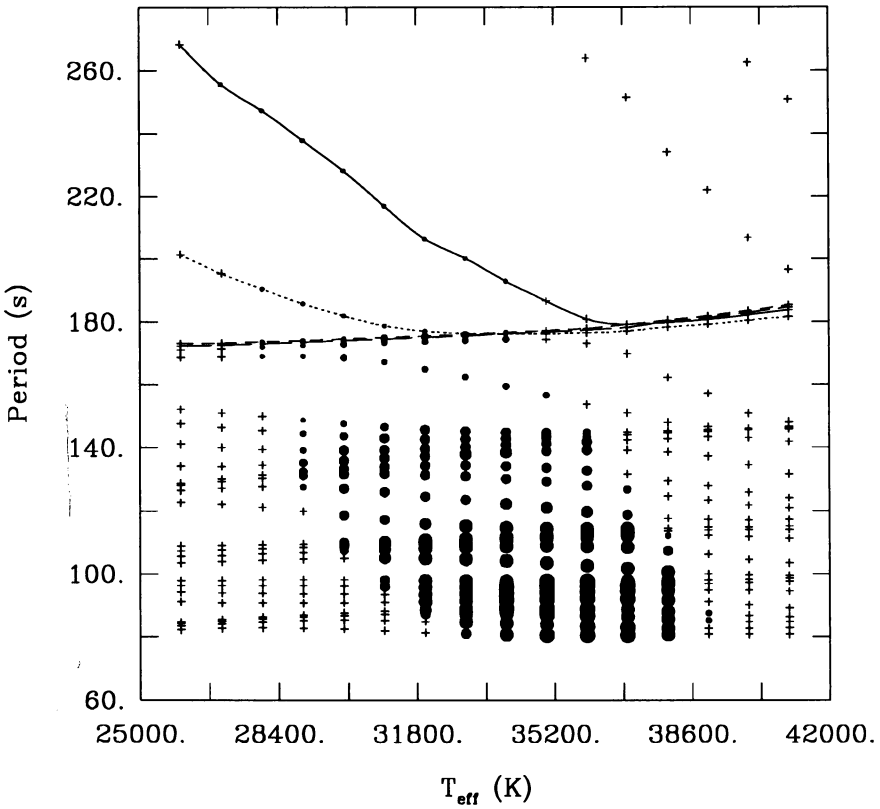

Figure 2. Period spectrum as a function of effective temperature for representative sdB models with $M = 0.48\ M_{\odot}$, log $g = 5.8$, and a H–rich envelope mass log $q(H) = -3.70$. All modes with $l = 0$, 1, 2, and 3, and with periods in the range 80–280 s are illustrated. A stable mode is represented by a small cross, while an excited mode is represented by a filled circle. There are 7 different sizes of filled circles, each size representing a range of values of the modulus of the imaginary part of the complex frequency, σ_i. In order of increasing circle size, the relevant values of σ_i (in Hz) are $< 10^{-7}$, $10^{-7} \leq \sigma_i < 5 \times 10^{-7}$, $5 \times 10^{-7} \leq \sigma_i < 10^{-6}$, $10^{-6} \leq \sigma_i < 5 \times 10^{-6}$, $5 \times 10^{-6} \leq \sigma_i < 10^{-5}$, $10^{-5} \leq \sigma_i < 5 \times 10^{-5}$, and $\geq 5 \times 10^{-5}$. The most unstable modes are thus those represented by the largest filled circles. The curves join together the fundamental modes and separate the p–modes from the g–modes in the diagram. The dashed (long–dashed, solid, dotted) curve joins together the modes with $l = 0$ and $k = 0$ ($l = 1$ and $k = 1$; $l = 2$ and $k = 0$; $l = 3$ and $k = 0$).

gravity EC14026 stars should show the longer periods (prediction #4).

Finally, one can also observe in the figure that the largest growth rates are found in the lowest gravity models. Insofar as linear theory may be relied upon, this suggests that the lower gravity EC14026 stars should show the larger amplitudes (prediction #5).

https://doi.org/10.1017/S0074180900238953 Published online by Cambridge University Press

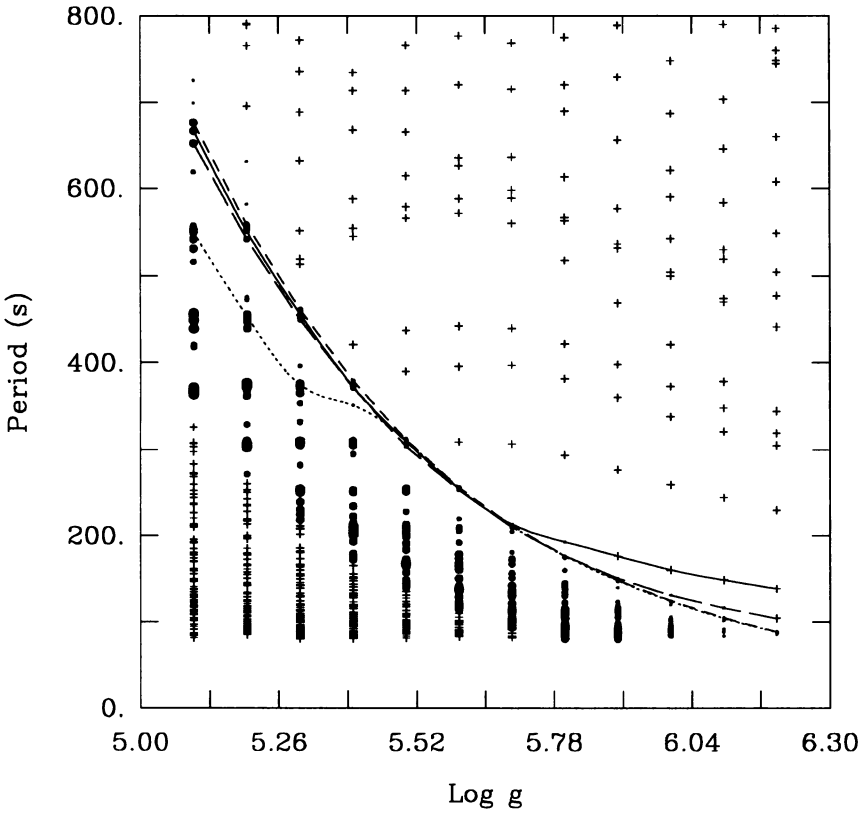

Figure 3. Period spectrum as a function of surface gravity for representative sdB models with $T_{\rm eff}$ = 34,000 K, $M = 0.48\ M_{\odot}$, and a H–rich envelope mass log $q(H) = -3.70$. All modes with $l = 0$, 1, 2, and 3, and with periods in the range 80–800 s are illustrated. As in Fig. 2, a stable mode is represented by a small cross, while an excited mode is represented by a filled circle. There are 5 different sizes of filled circles, each size representing a range of values of the modulus of the imaginary part of the complex frequency, σ_i. In order of increasing circle size, the relevant values of σ_i (in Hz) are $< 10^{-7}$, $10^{-7} \leq \sigma_i < 10^{-6}$, $10^{-6} \leq \sigma_i < 10^{-5}$, $10^{-5} \leq \sigma_i < 10^{-4}$, and $\geq 10^{-4}$. As in the previous figure, the most unstable modes are thus those represented by the largest filled circles. The curves join together the fundamental modes and separate the p–modes from the g–modes in the diagram. The dashed (dotted, solid, long–dashed) curve joins together the modes with $l = 0$ and $k = 0$ ($l = 1$ and $k = 1$; $l = 2$ and $k = 0$; $l = 3$ and $k = 0$).

5. Discussion and conclusion

The results of our nonadiabatic studies of models of sdB stars lead to definite predictions which can, in principle, be tested against the statistics of EC14026 stars. Although not enough statistics have accumulated on these objects yet, the few results available are very encouraging and tend to support strongly the

https://doi.org/10.1017/S0074180900238953 Published online by Cambridge University Press

reality of the destabilization mechanism we have uncovered in our models. For instance, the values of the periods of the modes discovered so far in EC14026 stars are *all* consistent with p–modes (prediction #3). Also, it turns out that the first 6 EC14026 stars discovered have very similar atmospheric parameters: $T_{\rm eff} \simeq 34{,}450$ K (450 K, rms deviation) and $\log g \simeq 5.85$ (0.09, rms deviation). This is the clustering of pulsators expected in the range 33,000–36,000 K for stars with these gravities (prediction #2). Their pulsation properties are also similar with periods found in the range 104–184 s and amplitudes of the individual modes ranging from a fraction of a millimag up to 14 millimag. We know of the existence of 2 other EC14026 stars: the recently discovered pulsator KPD2109+4401 (Billères et al. 1997), a star with $\log g \simeq 5.83$, but with a somewhat lower value $T_{\rm eff} \simeq 31{,}160$ K . In that case, the period range is pushed to somewhat higher values, 182–198 s, as expected for a cooler star (prediction #1). The case of PG1605+072 (Kilkenny, private communication) is even more interesting. This star currently stands out as an EC14026 object with a relatively low effective temperature, $T_{\rm eff} \simeq 30{,}000$ K, and, even more significantly, with a rather low surface gravity, $\log g \simeq 5.20$. As expected (prediction #4), the range of excited periods is broader and reaches values of up to 601 s. Also, the amplitude of the dominant mode at 482 s reaches a value of more than 24 millimag, the largest so far observed in EC14026 stars (prediction #5). Quite clearly, these results are rather encouraging, but must be seen as the first attempt to elucidate the asteroseismology of EC14026 stars, a field still in its infancy. For an update of the observational situation, the reader is referred to the interesting paper of Stobie et al. in these Proceedings.

References

Billères, M., Fontaine, G., Brassard, P., Charpinet, S., Liebert, J., Saffer, R.A., Bergeron, P., & Vauclair, G. 1997, *Ap.J.*, in press

Charpinet, S., Fontaine, G., Brassard, P., & Dorman, B. 1996, *Ap.J.*, **471**, L103

Charpinet, S., Fontaine, G., Brassard, P., Chayer, P., Rogers, F.J., Iglesias, C.A., & Dorman, B. 1997, *Ap.J.*, **483**, L123

Chayer, P., Fontaine, G., & Wesemael, F. 1995, *Ap.J.Suppl.*, **99**, 189

Dorman, B. 1995, in Proc. 32nd Liège Astrophysical Colloq., Stellar Evolution: What Should Be Done, ed. A. Noels, D. Fraipont-Caro, N. Grevesse, & P. Demarque (Liège: Institut d'Astrophysique), 291

Heber, U. 1991, in IAU Symposium 145, Evolution of Stars: The Photospheric Abundance Connection, ed. G. Michaud & A. Tutukov (Dordrecht: Kluwer), 363

Kilkenny, D., Koen, C., O'Donoghue, D., & Stobie, R.S. 1997, *M.N.R.A.S.*, **285**, 640

Koen, C., Kilkenny, D., O'Donoghue, D., Van Wyk, F., & Stobie, R.S. 1997, *M.N.R.A.S.*, **285**, 645

Michaud, G., Bergeron, P., Wesemael, F., & Fontaine, G. 1985, *Ap.J.*, **299**, 741

O'Donoghue, D., Lynas-Gray, A.E., Kilkenny, D., Stobie, R.S., & Koen, C. 1997, *M.N.R.A.S.*, **285**, 657

Saffer, R.A., Bergeron, P., Koester, D., & Liebert, J. 1994, *Ap.J.*, **432**, 351

Stobie, R.S., Kawaler, S.D., Kilkenny, D., O'Donoghue, D., & Koen, C. 1997, *M.N.R.A.S.*, **285**, 651